Nano Communication Networks 30 (2021) 100366

Contents lists available at ScienceDirect

Nano Communication Networks

journal homepage: www.elsevier.com/locate/nanocomnet

A fuzzy-logic-based fault detection system for medical Internet of Nano Things

Samane Sharif[a], Seyed Amin Hosseini Seno[a,*], Alireza Rowhanimanesh[b]

[a] Department of Computer Engineering, Ferdowsi University of Mashhad, P.O. Box: 9177948944, Mashhad, Iran
[b] Department of Electrical Engineering, University of Neyshabur, Neyshabur, Iran

ARTICLE INFO

Article history:
Received 22 February 2020
Received in revised form 14 July 2020
Accepted 29 July 2021
Available online 31 July 2021

Keywords:
Internet of Nano Things
Fault detection
Fuzzy logic
In silico study
Atherosclerosis

ABSTRACT

In this paper, a fuzzy-logic-based fault detection system is designed for a medical Internet of Nano Things architecture. The goal of this system is to detect the root cause and severity of the faults occurred in the in-body nanonetwork. Since nanomachines have very limited capabilities, the sampled data from the in-body nanonetwork is sent to cloud servers by means of an on-body micro-gateway. The fuzzy fault detection system was designed based on two well-known methods including Mamdani and Takagi–Sugeno–Kang (TSK) fuzzy systems. The performance of the proposed approach is evaluated on a theoretical model of medical in-body nanonetwork from the literature through in silico study. This nanonetwork includes eleven types of nanomachines which cooperate with each other within the arterial wall and interact with low-density lipoprotein (LDL), drug and signaling molecules in order to prevent the formation and development of Atherosclerosis plaques. Any fault in these nanomachines can highly take negative effect on treatment efficiency. The results of computer simulation and comparative study on 37 atherosclerosis patients demonstrate how the proposed approach could successfully detect the root cause and severity of the faults occurred in the nanonetwork.

1. Introduction

Nanotechnology, as a practical approach for miniaturization and construction of very small devices in nanoscale, provides new solutions in different areas including medicine, industry, biology, and military [1,2]. Particularly, medicine has been acquired significant advances with the aid of nanotechnology [3–6]. This recently emerging field is called nanomedicine, in which, nanomachines are able to noninvasively interact with body tissues and perform sensing and manipulation at cellular and molecular levels. A nanomachine is a basic functional unit with limited sensing and actuation abilities [1]. A nanonetwork is defined as a set of interacting nanomachines that exploits communication and cooperation among them to realize new synergic capabilities in contrast to a single nanomachine. Connecting nanonetworks to external networks such as the Internet has been a challenging topic over recent years. This new paradigm is called Internet of Nano Things (IoNT) [7]. Research works on IoNT can be divided into four general categories. The first category contains some articles that provide an overview of the IoNT and present open problems, challenges and future perspectives [8–10]. There still exist many challenges in the context of IoNT such as designing applicable methods for data collection from nanonetworks, optimizing the consumption of energy in micro-gateways, ensuring data privacy and security, developing a middleware layer to connect nanosensor networks to microscale devices and external networks, and creating appropriate service management systems for IoNT.

The second category focuses on the internal structure of nanomachines and their communication mechanism [11–18]. Nanomachines in molecular environments can communicate together and external devices in an appropriate manner. The third category is related to designing energy-aware communication protocols for nanomachines with low capabilities [19–21]. Computation-light scheduling algorithms is needed for access to communicating media. The last category puts an emphasis on the architecture of IoNT and different layers [22–25]. General architecture of IoNT consists of device, access and cloud layers. Cloud and access layers provide different resources for communicating, computation and caching requirements.

One of the promising applications of medical IoNT is drug delivery that can highly improve the therapeutic effectiveness and minimizes drug side effects. In medical IoNT, the occurrence of any fault in the in-body nanosensor network can significantly take negative effect on treatment efficiency. In this paper, a general fuzzy-logic-based fault detection approach is proposed for a specific architecture of medical IoNT based on two well-known design methods of fuzzy systems including Mamdani and Takagi–Sugeno–Kang (TSK). The goal of the fuzzy fault detection system

* Corresponding author.
E-mail address: hosseini@um.ac.ir (S.A. Hosseini Seno).

https://doi.org/10.1016/j.nancom.2021.100366
1878-7789/

is to detect the root cause and severity of the faults occurred in the in-body nanonetwork. Since nanomachines have very limited capabilities, the sampled data from the in-body nanonetwork is sent to cloud servers by means of an on-body micro-gateway. The performance of the proposed approach is evaluated on a theoretical model of medical in-body nanonetwork from the literature through in silico study on Atherosclerosis. The working environment of the nanonetwork is the interior of the wall of coronary arteries. The heart obtains its own supply of blood from these arteries. High accumulation of LDL (low-density lipoprotein) macromolecules in the wall of these arteries plays a crucial role in formation and development of atherosclerotic plaques and hardening of the arteries that is one of the main causes of heart attack.

This paper is organized as follows. In Section 2, a theoretical model of medical in-body nanonetwork, selected from the literature, is briefly introduced. Then, the details of the IoNT architecture are explained. In Section 3, a fuzzy-logic-based fault detection approach is proposed for this architecture. The performance of the proposed scheme is investigated through computer simulation in Section 4 and a comparative study is done. Finally, Section 5 concludes the paper.

2. The architecture of medical IoNT

As depicted in Fig. 1, the IoNT architecture is composed of three layers including *device*, *access* and *cloud* layers. The device layer is the lowest layer comprising of in-body nanosensor networks and body-area micro-gateway. The access layer, as a middle layer, supports communication between the device and cloud layers via user terminals and access points. The cloud layer is the highest layer which consists of various servers and data centers responsible for storage and processing of collected data.

As nanosensor network, a theoretical model of medical in-body nanonetwork has been selected from the literature [12]. There are many papers in the literature that have used this model in their research [26–31]. This nanonetwork has been designed based on the notion of swarm control systems for nanomedicine as a universal approach for performing complex in-body therapeutical tasks at nanoscale [12]. Although each nanomachine has very limited capability of sensing, computing, and actuation, a huge number of them can be injected within the body. As a promising approach, the above-mentioned notion exploits the cooperation and communication among nanomachines to realize swarm intelligence at nanoscale.

Fig. 2 illustrates the schematic representation of the in-body nanonetwork [12]. The working environment is the interior of the arterial wall of coronary arteries, in which high accumulation of LDL macromolecules, ∼22 nm in diameter, plays a crucial role in formation and development of atherosclerotic plaques as one of the main causes of heart attack. The nanonetwork employs the idea of swarm fuzzy feedback control, described with details in [12,26], to reduce the LDL level inside the arterial wall through intelligent drug delivery. In this idea, a conventional fuzzy controller can be microscopically implemented in the aqueous environment of living tissue by a swarm of very simple nanomachines, called Fuzzy Nanoparticles (FNP), in a collective manner. The universality, scalability, and robustness of this approach have been demonstrated in [12]. If the fuzzy controller has N fuzzy if-then rules, N types of FNPs are required, such that the FNPs of type j are responsible for realizing the jth rule. Due to toxicity and other clinical issues, there is a hard constraint on the maximum allowed dosage of FNPs that can be injected in the blood. Since there are N types of FNPs, the dosage of each type of FNPs will become very low for large values of N. As the reservoir capacity of each FNP is very small, and at each time instant, only few number of fuzzy rules will be fired, FNPs will not be efficient for releasing drug. Instead, FNPs release a signaling molecule called pheromone which excites the actuator nanomachines called Auxiliary Nanoparticles (ANPs) that are used for drug delivery.

In this study, similar to [12], there exist 10 types of FNP nanomachines, i.e. $\{FNP1, FNP2, \dots, FNP10\}$. An FNP of type j consists of a nanoscale molecular concentration sensor for taking feedback from LDL concentration and a computing unit for implementing the jth fuzzy rule. This computing unit manipulates a controllable molecular pump, connected to a pheromone reservoir, to adjust the pheromone release rate of FNP. It has been proven in [12] that the swarm of these N types of FNPs could collectively realize the equivalent mapping of the given fuzzy controller between LDL (input) and Pheromone (output) in the aqueous environment of the tissue at nanoscale. Now, in order to transduce the pheromone signal to drug signal, ANPs are used as the actuator nanomachines. Drug delivery is the task of ANP nanomachines which are simpler than FNPs. Each ANP senses the level of pheromone diffused by FNPs in the environment and consists of a controllable nanometer-sized valve connected to a drug reservoir. The drug release rate of this valve is linearly proportional to the measured level of pheromone. The structure of FNPs and ANPs are schematically shown in Fig. 2.

Fig. 3a schematically depicts the anatomical structure of the arterial wall. In most of the robust mathematical models for macromolecule transport in the arterial wall, the arterial wall is partitioned into four important physiological layers due to their thickness and the effect of their cellular and molecular structure on creation and growth of atherosclerotic plaques and hardening of the arteries.

These four layers includes endothelium, intima, IEL (internal elastic lamina), and media [32]. The thickness of each wall layer is shown in Fig. 3b. The nanonetwork employs eleven types of cooperating nanomachines (ANP and 10 types of FNP) which interact with LDL, drug, and signaling molecule (pheromone) in order to reduce the LDL level in all layers of the arterial wall and ultimately prevent the formation and development of atherosclerosis plaques. The mathematical model of diffusion–advection–reaction for these interacting nano-agents are described by the following nonlinear partial differential equations [12]:

$$\frac{\partial c^l_{LDL}}{\partial t} = -\left(1-\sigma^l_{fLDL}\right) V_{filt} \nabla c^l_{LDL} + D^l_{LDL} \nabla^2 c^l_{LDL} - k^l_{rLDL} c^l_{LDL} - R_y(c^l_{LDL}, c^l_{drug}) \quad (1)$$

$$\frac{\partial c^{lj}_{FNP}}{\partial t} = -\left(1-\sigma^l_{fFNP}\right) V_{filt} \nabla c^{lj}_{FNP} + D^l_{FNP} \nabla^2 c^{lj}_{FNP} - k^l_{rFNP} c^{lj}_{FNP} \quad (j = 1, \dots, \mathrm{N}) \quad (2)$$

$$\frac{\partial c^l_{ph}}{\partial t} = -\left(1-\sigma^l_{fph}\right) V_{filt} \nabla c^l_{ph} + D^l_{ph} \nabla^2 c^l_{ph} - k^l_{rph} c^l_{ph} + m_{ph} \sum_{j=1}^{N} c^{lj}_{FNP} u^{lj}_{FNP} \quad (3)$$

$$\frac{\partial c^l_{ANP}}{\partial t} = -\left(1-\sigma^l_{fANP}\right) V_{filt} \nabla c^l_{ANP} + D^l_{ANP} \nabla^2 c^l_{ANP} - k^l_{rANP} c^l_{ANP} \quad (4)$$

$$\frac{\partial c^l_{drug}}{\partial t} = -\left(1-\sigma^l_{fdrug}\right) V_{filt} \nabla c^l_{drug} + D^l_{drug} \nabla^2 c^l_{drug} - k^l_{rdrug} c^l_{drug} - R_z\left(c^l_{LDL}, c^l_{drug}\right) + m_{drug} c^l_{ANP} u^l_{ANP} \quad (5)$$

$$u^{lj}_{FNP} = \overline{P}_j \mu_{A_j}\left(c^l_{LDL}\right) \quad (6)$$

$$u^l_{ANP} = k_{ANP} c^l_{ph} \quad (7)$$

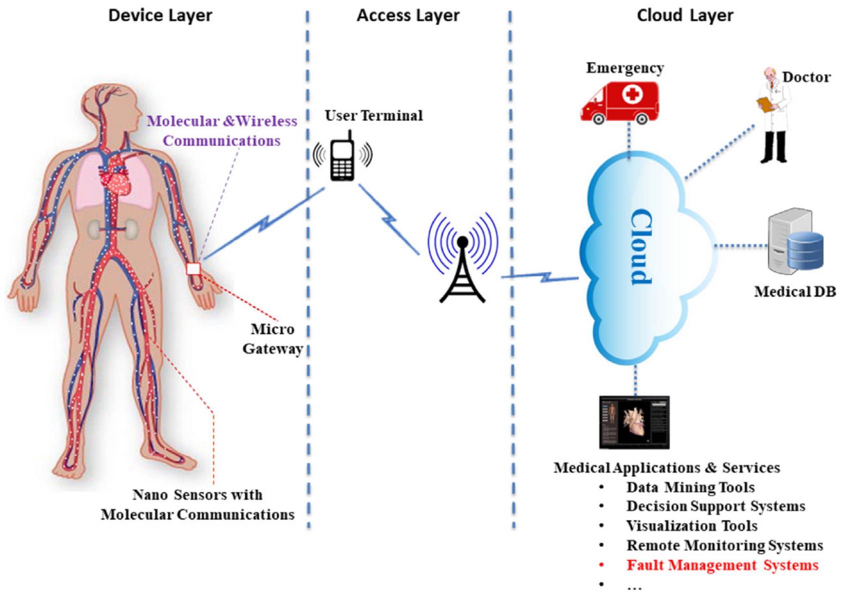

Fig. 1. The architecture of medical IoNT.

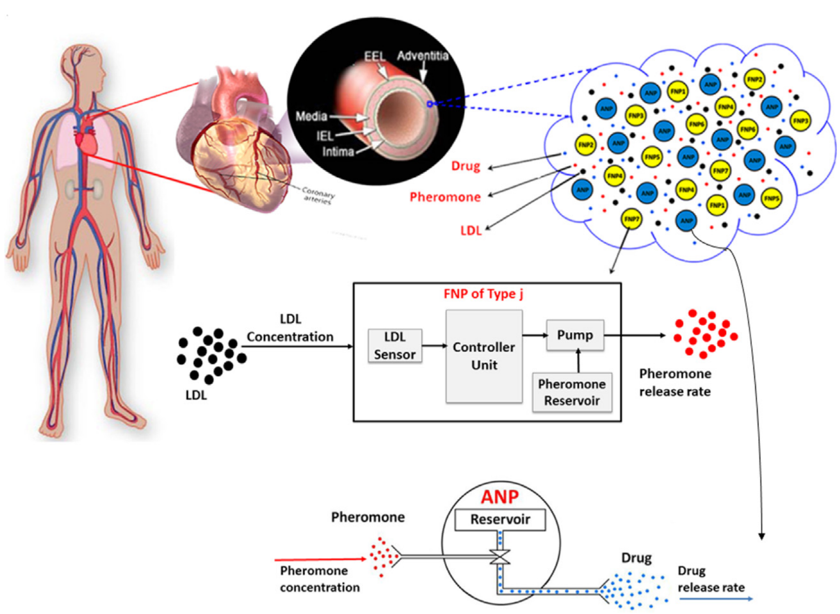

Fig. 2. The in-body nanonetwork and the internal structure of nanomachines (inspired from [12]).

where l is the layer number (from endothelium ($l = 1$) to media ($l = 4$)), ∇ the gradient, ∇^2 the Laplacian, c^l_{LDL} the concentration of LDL molecules, V_{filt} the filtration velocity, σ^l_{fLDL} the filtration reflection coefficient, D^l_{LDL} the effective diffusivity, k^l_{rLDL} the reaction coefficient, m_{LDL} the mass of LDL molecule, and R_y and R_z are the functions of LDL-drug reaction in the lth layer. Similar notation is used for other nano-agents. u^{lj}_{FNP} and u^l_{ANP} are the pheromone and drug release rates (molecule s^{-1}) by FNP of type j and ANP, respectively. μ_{A_j}, $\overline{P}_j$ and k_{ANP} are design parameters of nanomachines. FNP (and ANP), LDL and drug (and pheromone) are assumed to be spherical particles of 100 nm, 22 nm and 4 nm in diameter, respectively.

Eq. (1) computes the temporal and spatial changes of LDL concentration. The four terms in the right of this equation represent the effects of advection, diffusion, clearance, and reaction between drug and LDL, respectively. Similar terms and notations are available in the Eqs. (2)–(5) for other nano-agents. In Eq. (3), the last term in the right of equation describes the collective release rate of pheromone from N types of FNP nanomachines. Similarly, the last term in the right of Eq. (5) shows the drug release rate from ANP nanomachines. Eq. (6) demonstrates how an FNP of type j implements the jth fuzzy rule (the relation between pheromone release rate by an FNP of type j and its sensed LDL level). Finally, Eq. (7) shows that an ANP nanomachine acts as a linear proportional actuator (the relation between the drug release rate by an ANP and its sensed pheromone level).

Some assumptions of the model are as follows. In this model, glycocalyx is ignored because of its small thickness (60 nm), and the effect of adventitia is modeled in boundary conditions. For simplicity, the effect of LDL concentration on fluid velocity is

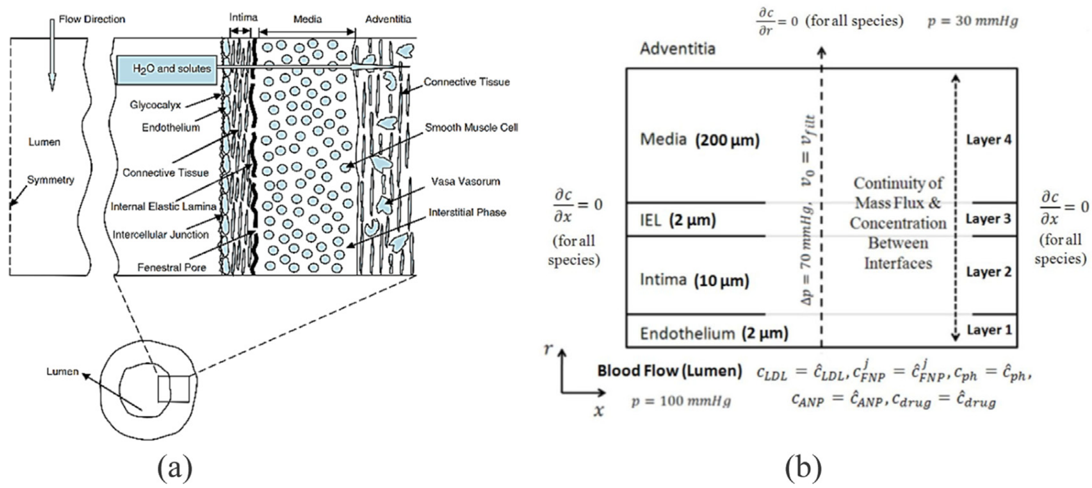

Fig. 3. (a) The anatomical structure of the arterial wall [32], (b) The boundary conditions of the mathematical model [26].

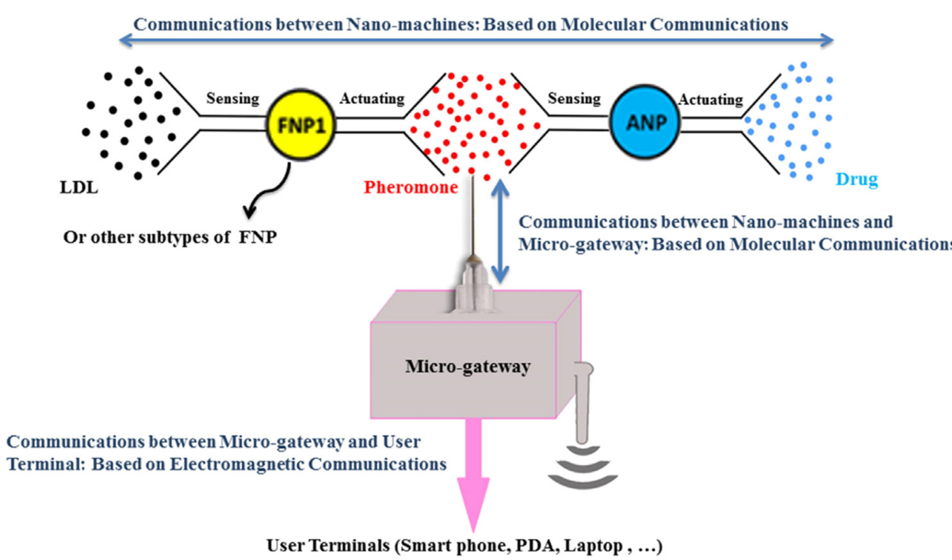

Fig. 4. The communication between nanomachines and micro-gateway.

neglected, and fluid velocity is assumed to be constant in all wall layers and equal to filtration velocity. The boundary conditions have been represented in Fig. 3b. For the boundary conditions at the interfaces between wall layers, the continuity of mass flux and concentration is considered. More details have been discussed in [12,28].

The nanonetwork of Fig. 2 benefits from molecular communication, in which nanomachines can react to particular molecules as a received message (receive) and release other specific molecules as a response (send). Fig. 4 shows the communication between nanomachines and micro-gateway. As displayed in this figure, the micro-gateway has a mechanical module such as a micro-needle to periodically take sample from the level of pheromone molecules in blood. Then, it sends these data to the user terminal (smart phone, laptop, etc.) via a wireless transceiver. The user terminal connects to an access point to transmit these data to the cloud servers.

Sending the nanonetwork data to the cloud provides an opportunity to exploit computational resources of cloud for advanced data processing such as intelligent fault detection of nanonetwork that is the goal of this paper. There exist many reasons for developing fault management system based on cloud resources. First, cloud-based fault management makes remote monitoring and decision making possible. Second, the nanometer-sized sensors used in nanosensor networks have many limitations in processing, storage, and communication capabilities. As an alternative, these computational requirements can be executed on cloud resources. Third, different healthcare centers can share their collected data through cloud and such data can be furtherly employed for better diagnosis and prognosis.

3. Fuzzy-logic-based fault detection

Fuzzy logic is a universal model-free approach for modeling, analysis, and control of complex systems in the presence of uncertainty. Since fuzzy logic is close to human perception and it can efficiently exploit expert linguistic knowledge as well as mathematical analysis, it is a very appropriate for designing medical decision support systems. The most well-known fuzzy systems are Mamdani and TSK (Takagi–Sugeno–Kang) [33]. A Mamdani fuzzy system is usually designed linguistically using expert knowledge, while a TSK fuzzy system is typically designed through data analysis and mathematical optimization. In this

Table 1
The fuzzy rules defined by expert in the knowledge base of the Mamdani fuzzy system.

Rule index (f)	Fuzzy if-then rule
Rule 1:	If ERR is zero and PRO is very similar then RC is no fault and S is low
Rule 2:	If ERR is small and PRO is very similar then RC is FNP123 and S is average
Rule 3:	If ERR is medium and PRO is similar then RC is FNP8910 and S is low
Rule 4:	If ERR is medium and PRO is very similar then RC is FNP4567 and S is average
Rule 5:	If ERR is large and PRO is different then RC is FNP8910 and S is average
Rule 6:	If ERR is large and PRO is fairly different then RC is ANP and S is average
Rule 7:	If ERR is large and PRO is fairly similar then RC is ANP and S is average
Rule 8:	If ERR is very large and PRO is very different then RC is FNP8910 and S is high
Rule 9:	If ERR is very large and PRO is different then RC is ANP and S is high
Rule 10:	If ERR is very large and PRO is fairly different then RC is ANP and S is average

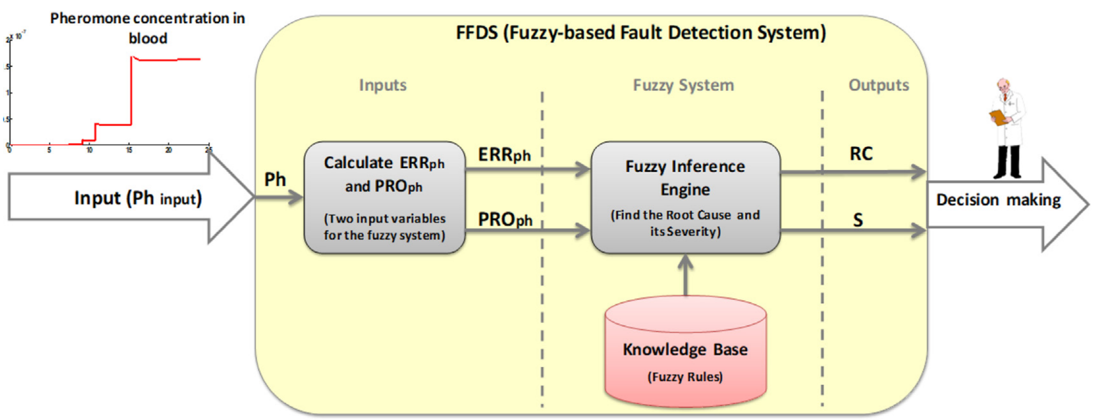

Fig. 5. The structure of the proposed fuzzy fault detection system.

section, these two approaches are employed to design two fuzzy-logic-based fault detection systems to detect the root cause and severity of the faults occurred in the nanonetwork. A comparative study is performed in the next section through computer simulation.

Fig. 5 the general structure of the proposed fuzzy fault detection system. In this figure, the input signal, Ph_{input}, is the pheromone level sampled over time from patient in-body nanonetwork by the micro-gateway. Also, the normal signal, Ph_{Normal}, is defined as the desired signal of pheromone level when the treatment process is performed normally and no fault is occurred in nanomachines. The error metrics ERR_{ph} and PRO_{ph} is calculated as the difference and proportion between the normal signal ($Ph_{Normal}(\mathrm{n})$) and the input signal ($Ph_{input}(\mathrm{n})$) for a specific time interval:

$$ERR_{ph} = \frac{\sum_{n=1}^{N_s} (Ph_{Normal}(\mathrm{n}) - Ph_{input}(\mathrm{n}))^2}{\sum_{i=1}^{N_s} (Ph_{Normal}(\mathrm{n}))^2} \tag{8}$$

$$PRO_{ph} = \frac{1}{N_s} \sum_{n=1}^{N_s} \frac{Ph_{input}(\mathrm{n})}{Ph_{Healthy}(\mathrm{n})} \tag{9}$$

where N_s is the number of samples in a specific time interval which can be adjusted by physician depending on the patient conditions. The range of the above metrics is between 0 and 1. Here, the ten types of FNP nanomachines available in the in-body nanonetwork are categorized into three groups based on the importance of their roles in drug delivery and their effects on the error metrics . These three groups as well as the group of ANPs provides four categories of nanomachines: {ANP}, {FNPs of types 1,2,3}, {FNPs of types 4,5,6,7}, and {FNPs of types 8,9,10}. FNPs of types 8,9,10 have more effect on releasing drug. In the rest of this section, two fuzzy fault detection systems are designed suing Mamdani and TSK fuzzy systems.

3.1. Mamdani fuzzy system

According to expert knowledge, 10 fuzzy if-then rules have been linguistically defined in Table 1 in the following form:

Rule f: If *ERR* is A_{i_f} and *PRO* is B_{j_f} then *RC* is C_{k_f} and *S* is D_{l_f} where *ERR* and *PRO* are the inputs of the fuzzy system, *RC* and *S* are respectively the root cause and severity of the occurred fault and the outputs of the fuzzy system, i_f, j_f, k_f and l_f are the indices of the fuzzy sets corresponding to the linguistic words used in the antecedent and consequent parts of the f$^{\text{th}}$ rule in Table 1. These fuzzy sets including A, B, C, and D are displayed in Fig. 6. Due to generality and computational simplicity, triangular membership functions are used. Using Mamdani fuzzy inference engine and centers average defuzzifier [33], the fuzzy system computes the root cause (RC) and severity (S) of the occurred fault as:

$$RC = \frac{\sum_{\mathrm{f}=1}^{10} \mu_{A_{i_f}}\left(ERR_{ph}\right) * \mu_{B_{j_f}}\left(PRO_{ph}\right) {}^{*}\bar{C}_{k_f}}{\sum_{\mathrm{f}=1}^{10} \mu_{A_{i_f}}\left(ERR_{ph}\right) * \mu_{B_{j_f}}\left(PRO_{ph}\right)} \tag{10}$$

$$S = \frac{\sum_{\mathrm{f}=1}^{10} \mu_{A_{i_f}}\left(ERR_{ph}\right) * \mu_{B_{j_f}}\left(PRO_{ph}\right) {}^{*}\bar{D}_{l_f}}{\sum_{\mathrm{f}=1}^{10} \mu_{A_{i_f}}\left(ERR_{ph}\right) * \mu_{B_{j_f}}\left(PRO_{ph}\right)} \tag{11}$$

where f is the index of rule, $\mu_{A_{i_f}}(.)$ and $\mu_{B_{j_f}}(.)$ are the membership functions of the fuzzy sets A_{i_f} and B_{j_f}, and $\bar{C}_{k_f}$ and $\bar{D}_{k_f}$ are the center of the fuzzy sets C_{k_f} and D_{k_f}, respectively. *RC* should be rounded to determine the recognized root cause, where '0' means 'No Fault', 1: 'ANPs are faulty', 2: 'FNPs of types 1,2,3 are faulty', 3: 'FNPs of types 4,5,6,7 are faulty', and 4: 'FNPs of types 8,9,10 are faulty'. The severity (*S*) is defined as the degree of severity of the occurred fault that is a real number between 0 and 1. For example, the severity degree of 0.2 means that approximately 20% of nanomachines are faulty in the recognized category. Once the root cause and the severity of an occurred fault is recognized by the system, medical team can make a better

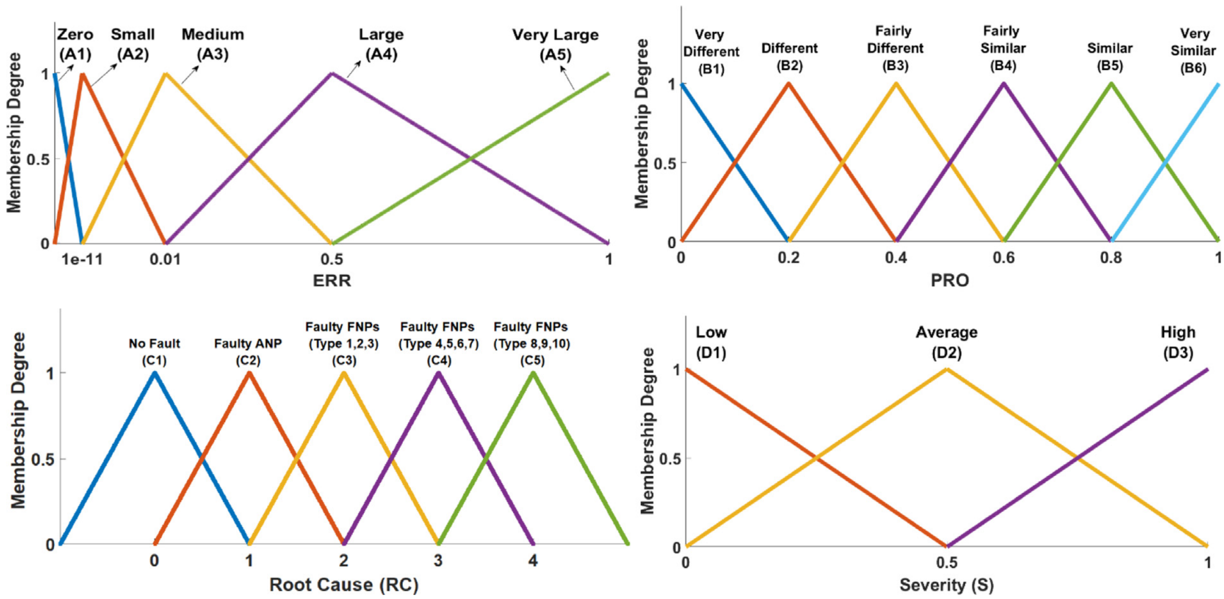

Fig. 6. The defined fuzzy sets over the inputs (ERR and PRO) and outputs (RC and S) of the Mamdani fuzzy system.

decision for improving the treatment efficiency such as injecting additional nanomachines of some categories into the patient's body to return the treatment process to its normal state. This injection can be done manually by a clinician, or automatically via an on-body infusion pump that is connected to the cloud for receiving control commands.

3.2. TSK fuzzy system

In contrast to the Mamdani fuzzy fault detection system of the previous section that was designed linguistically based on expert knowledge, in this section a TSK fuzzy fault detection system is designed based on data analysis and mathematical optimization. The format of a TSK fuzzy if-then rule is as follows:

If ERR is A_i and PRO is B_j then $RC = \overline{U}_{ij}$ and $S = \overline{V}_{ij}$

where A_i and B_j are the fuzzy sets defined in Fig. 6. Since there are 5 fuzzy sets over ERR (i.e. $i = 1, \ldots, 5$) and 6 fuzzy sets over PRO (i.e. $j = 1, \ldots, 6$), the total number of fuzzy rules is 30. $\overline{U}_{ij}$ and $\overline{V}_{ij}$ are the real constant parameters of the consequent part of the rules that are initially unknown and should be found through data analysis and optimization. Using TSK fuzzy inference engine [33], the fuzzy system computes the root cause (RC) and severity (S) of the occurred fault as:

$$RC = \frac{\sum_{i=1}^{3}\sum_{j=1}^{6}\mu_{A_i}\left(ERR_{ph}\right)*\mu_{B_j}\left(PRO_{ph}\right)*\overline{U}_{ij}}{\sum_{i=1}^{3}\sum_{j=1}^{6}\mu_{A_i}\left(ERR_{ph}\right)*\mu_{B_j}\left(PRO_{ph}\right)} \tag{12}$$

$$S = \frac{\sum_{i=1}^{3}\sum_{j=1}^{6}\mu_{A_i}\left(ERR_{ph}\right)*\mu_{B_j}\left(PRO_{ph}\right)*\overline{V}_{ij}}{\sum_{i=1}^{3}\sum_{j=1}^{6}\mu_{A_i}\left(ERR_{ph}\right)*\mu_{B_j}\left(PRO_{ph}\right)} \tag{13}$$

Assume that the dataset includes P faulty cases, where the true values of the root cause and severity for each case are RC_T^p and S_T^p, respectively, where $p = 1, \ldots, P$. Also, RC^p and S^p are the estimated values of the root cause and severity of the pth case by the TSK fuzzy system through Eqs. (12)–(13). Here, the following two optimization problems, in the form of minimization of the mean square error (MSE), are designed to find the optimal values of the unknown parameters of the TSK fuzzy system:

$$\min_{\overline{U}=\{\overline{U}_{ij}|i=1,\ldots,5,j=1,\ldots,6\}} \frac{1}{P}\sum_{p=1}^{P}(RC_T^p - RC^p)^2 \tag{14}$$

s.t. $\overline{U}_{Min} \le \overline{U}_{ij} \le \overline{U}_{Max}$, $i = 1, \ldots, 5, j = 1, \ldots, 6$

$$\min_{\overline{V}=\{\overline{V}_{ij}|i=1,\ldots,5,j=1,\ldots,6\}} \frac{1}{P}\sum_{p=1}^{P}(S_T^p - S^p)^2 \tag{15}$$

s.t. $\overline{V}_{Min} \le \overline{V}_{ij} \le \overline{V}_{Max}$, $i = 1, \ldots, 5, j = 1, \ldots, 6$

where $\overline{U}_{Min}$, $\overline{U}_{Max}$, $\overline{V}_{Min}$, and $\overline{V}_{Max}$ are the lower and upper bounds for $\overline{U}_{ij}$ and $\overline{V}_{ij}$, respectively. We used Optimization Toolbox in MATLAB to solve these optimization problems (Eqs. (14) and (15)). The results are discussed in the next section.

4. In silico study

In this section, the performance of the proposed approach is evaluated on 37 atherosclerosis patients with distinguishing faults in their therapeutical in-body nanonetworks through computer simulation in MATLAB. Particularly, the nanonetwork has been simulated with the aid of ADENP tool, developed in [26], which solves the nonlinear partial differential equations of the mathematical model of Section 2. These randomly generated faulty cases include all 4 categories of root causes with different degrees of severity from 0 to 1. The micro-gateway takes sample from the pheromone level of blood every 10 s and sends these data to the cloud resources via middle layer. Fig. 7 shows the received pheromone signals from the in-body nanonetwork of four examples of faulty cases in comparison with the normal pheromone signal during 24 h.

Table 2 depicts the accuracy evaluation of the proposed fuzzy fault detection system using Mamdani and TSK approaches. The accuracy of root cause detection and severity estimation are calculated in terms of $(True/Total) * 100\%$ and $(1 - MAE) * 100\%$, respectively. $True$ is number of true detections, $Total$ is the total number of cases, and MAE stands for mean absolute error. The accuracy of root cause detection (severity estimation) is 72.97% (83.11%) and 81.08% (87.25%) in Mamdani and TSK, respectively. According to these results, TSK fuzzy system has more accurate performance in contrast to Mamdani. But on the other hand, the computational complexity of TSK fuzzy system is more than Mamdani due to the number of fuzzy rules, that is 30 in TSK but 10 in Mamdani. Also, since Mamdani fuzzy system is designed linguistically, it is more interpretable by clinical experts.

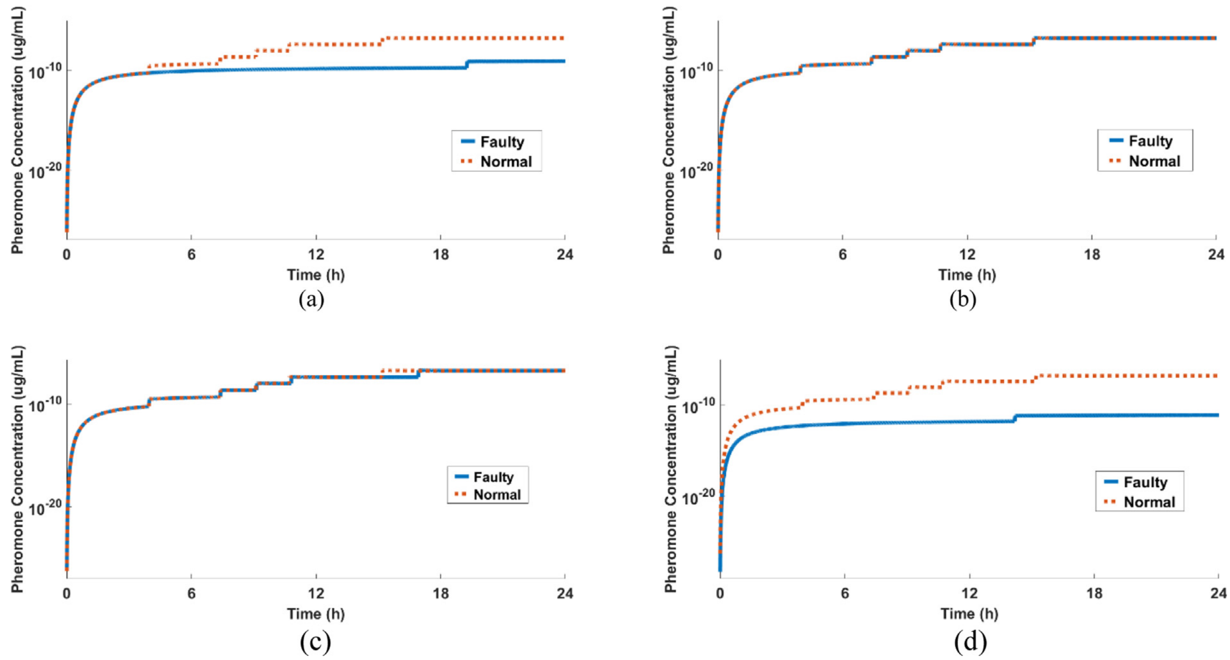

Fig. 7. The received pheromone signals from the in-body nanonetwork of four examples of faulty cases in comparison with the normal pheromone signal during 24 h. The vertical axis is in log scale. (a) 'Faulty ANPs' with severity of 0.98, (b) 'Faulty FNPs of type 1,2,3' with severity of 0.5, (c) 'Faulty FNPs of type 4,5,6,7' with severity of 0.5, (d) 'Faulty FNPs of type 8,9,10' with severity of 0.09.

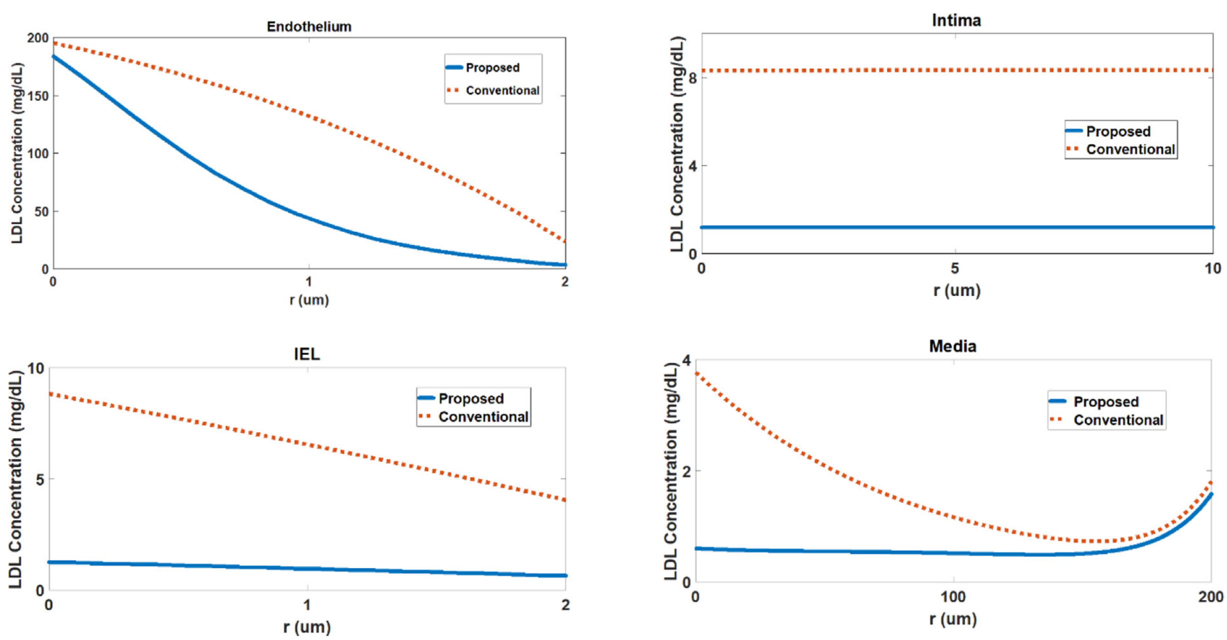

Fig. 8. The spatial profiles of LDL level in four layers of arterial wall at steady state in the presence of random faults: The conventional nanonetwork of Ref. [26] (dotted) vs. the proposed nanonetwork (solid).

Table 2
Accuracy evaluation of the proposed fuzzy fault detection system.

Accuracy	Approach	
	Mamdani	TSK
Root cause detection	72.97%	81.08%
Severity estimation	83.11%	87.25%

In order to show how the proposed fuzzy fault detection system can improve the robust performance of the medical treatment process, a test scenario is discussed here and the robustness of the performance of the in-body nanonetwork equipped by the proposed fuzzy fault detection system is compared with the conventional in-body nanonetwork of Ref. [26]. The faulty case is Example 'a' of Fig. 7 in which the ANP nanomachines are severely faulty with severity degree of 0.98. The proposed approach could accurately detect the fault and its severity. Accordingly, the clinical supervisor injects an appropriate compensatory dosage of ANP nanomachines into the patient's body. Fig. 8 compares the spatial profiles of LDL level within four layers of arterial wall at steady state after 24 h for the conventional nanonetwork of

Ref. [26] (dotted) and the proposed nanonetwork (solid). It is clear that in conventional nanonetwork, the LDL level could not be efficiently reduced due to the occurred fault, while in the proposed nanonetwork, the effect of the occurred fault could be efficiently compensated and the performance returned to normal. In general, the results demonstrated that the proposed fuzzy fault detection system could improve the robustness and reliability of medical IoNT.

5. Conclusion

The goal of this paper is to use the notion of fuzzy-logic-based fault detection for medical Internet of Nano Things. Since nanomachines have very limited capabilities, the sampled data from the in-body nanonetwork is transmitted to cloud servers via a micro-gateway located on body area. The task of the fault detection system is to detect the root cause and severity of the faults occurred in the nanomachines. The proposed fuzzy fault detection system was developed based on two well-known methods including Mamdani and TSK. The Mamdani fuzzy system was designed linguistically according to expert knowledge, while TSK fuzzy system was designed through data analysis and mathematical optimization. The performance of the proposed approach was evaluated on a theoretical model of medical in-body nanonetwork from the literature through in silico study. This nanonetwork includes eleven types of nanomachines which cooperate within the arterial wall and interact with LDL, drug, and signaling molecules in order to prevent the formation and development of atherosclerotic plaques. Different kinds of faults with different degrees of severity were generated randomly in the in-body nanonetworks of 37 atherosclerosis patients in computer simulation. The accuracy of root cause detection (severity estimation) was 72.97% (83.11%) and 81.08% (87.25%) in Mamdani and TSK, respectively. The total number of fuzzy rules was 10 in Mamdani and 30 in TSK. Also, the robustness of the nanonetwork equipped by the proposed fuzzy fault detection system was compared with the conventional nanonetwork in the literate. The results demonstrated that the proposed approach could enhance the robustness and reliability of medical IoNT.

CRediT authorship contribution statement

Samane Sharif: Internet of nano things, Fault management, Fuzzy logic. **Seyed Amin Hosseini Seno:** Internet of nano things, Fault management. **Alireza Rowhanimanesh:** Medical nanonetwork, In silico study, Systems biology.

Declaration of competing interest

The authors declare that they have no known competing financial interests or personal relationships that could have appeared to influence the work reported in this paper.

References

[1] I.F. Akyildiz, F. Brunetti, C. Blázquez, Nanonetworks: A new communication paradigm, Comput. Netw. 52 (12) (2008) 2260–2279.
[2] I.F. Akyildiz, J.M. Jornet, Electromagnetic wireless nanosensor networks, Nano Commun. Netw. 1 (1) (2010) 3–19.
[3] L. Felicetti, M. Femminella, G. Reali, P. Liò, Applications of molecular communications to medicine: A survey, Nano Commun. Netw. 7 (2016) 27–45.
[4] Y. Chahibi, Molecular communication for drug delivery systems: A survey, Nano Commun. Netw. 11 (2017) 90–102.
[5] M. Stelzner, F. Dressler, S. Fischer, Function centric nano-networking: Addressing nano machines in a medical application scenario, Nano Commun. Netw. 14 (2017) 29–39.
[6] J.L. Marzo, J.M. Jornet, M. Pierobon, Nanonetworks in biomedical applications, Curr. Drug Targets 20 (8) (2019) 800–807.
[7] I.F. Akyildiz, J.M. Jornet, The internet of nano-things, IEEE Wirel. Commun. 17 (6) (2010) 58–63.
[8] S. Balasubramaniam, J. Kangasharju, Realizing the internet of nano things: challenges, solutions, and applications, Computer 46 (2) (2012) 62–68.
[9] A. Nayyar, V. Puri, D.N. Le, Internet of nano things (IoNT): Next evolutionary step in nanotechnology, Nanosci. Nanotechnol. 7 (1) (2017) 4–8.
[10] M.H. Miraz, M. Ali, P.S. Excell, R. Picking, Internet of nano-things, things and everything: future growth trends, Future Internet 10 (8) (2018) 68.
[11] I.F. Akyildiz, M. Pierobon, S. Balasubramaniam, Y. Koucheryavy, The internet of bio-nano things, IEEE Commun. Mag. 53 (3) (2015) 32–40.
[12] A. Rowhanimanesh, Swarm Control Systems for Nanomedicine and Its Application To the Prevention of Atherosclerosis (Doctoral dissertation of Control Engineering), Ferdowsi University of Mashhad, 2013.
[13] M. Gregori, I.F. Akyildiz, A new nanonetwork architecture using flagellated bacteria and catalytic nanomotors, IEEE J. Sel. Areas Commun. 28 (4) (2010) 612–619.
[14] T. Nakano, T. Suda, Y. Okaie, M.J. Moore, A.V. Vasilakos, Molecular communication among biological nanomachines: A layered architecture and research issues, IEEE Trans. Nanobiosci. 13 (3) (2014) 169–197.
[15] U.A. Chude-Okonkwo, R. Malekian, B.T. Maharaj, Biologically inspired bio-cyber interface architecture and model for Internet of bio-nanothings applications, IEEE Trans. Commun. 64 (8) (2016) 3444–3455.
[16] M. Kuscu, O.B. Akan, Modeling convection–diffusion-reaction systems for microfluidic molecular communications with surface-based receivers in Internet of Bio-Nano Things, PLoS One 13 (2) (2018) e0192202.
[17] P.K.D. Pramanik, A. Solanki, A. Debnath, A. Nayyar, S. El-Sappagh, K.S. Kwak, Advancing modern healthcare with nanotechnology, nanobiosensors, and internet of nano things: Taxonomies, applications, architecture, and challenges, IEEE Access 8 (2020) 65230–65266.
[18] H. Fouad, M. Hashem, A.E. Youssef, A nano-biosensors model with optimized bio-cyber communication system based on Internet of Bio-Nano Things for thrombosis prediction, J. Nanopart. Res. 22 (7) (2020) 1–17.
[19] N. Akkari, P. Wang, J.M. Jornet, E. Fadel, L. Elrefaei, M.G.A. Malik, S. Almasri, I.F. Akyildiz, Distributed timely throughput optimal scheduling for the Internet of Nano-Things, IEEE Internet Things J. 3 (6) (2016) 1202–1212.
[20] F. Al-Turjman, A cognitive routing protocol for bio-inspired networking in the Internet of Nano-Things (IoNT), Mob. Netw. Appl. (2017) 1–15.
[21] F. Afsana, M. Asif-Ur-Rahman, M.R. Ahmed, M. Mahmud, M.S. Kaiser, An energy conserving routing scheme for wireless body sensor nanonetwork communication, IEEE Access 6 (2018) 9186–9200.
[22] F. Dressler, S. Fischer, Connecting in-body nano communication with body area networks: Challenges and opportunities of the Internet of Nano Things, Nano Commun. Netw. 6 (2) (2015) 29–38.
[23] G. Piro, G. Boggia, L.A. Grieco, On the design of an energy-harvesting protocol stack for Body Area Nano-NETworks, Nano Commun. Netw. 6 (2) (2015) 74–84.
[24] A. Galal, X. Hesselbach, Nano-networks communication architecture: Modeling and functions, Nano Commun. Netw. 17 (2018) 45–62.
[25] S. Sicari, A. Rizzardi, G. Piro, A. Coen-Porisini, L.A. Grieco, Beyond the smart things: Towards the definition and the performance assessment of a secure architecture for the Internet of Nano-Things, Comput. Netw. 162 (2019) 106856.
[26] A. Rowhanimanesh, M.R. Akbarzadeh-T, Stigmergic cooperation of nanoparticles for swarm fuzzy control of low-density lipoprotein concentration in the arterial wall, Appl. Soft Comput. 34 (2015) 799–812.
[27] A. Rowhanimanesh, M.R. Akbarzadeh-T, Control of low-density lipoprotein concentration in the arterial wall by proportional drug-encapsulated nanoparticles, IEEE Trans. Nanobiosci. 11 (4) (2012) 394–401.
[28] A. Rowhanimanesh, M.R. Akbarzadeh Totonchi, Autonomous drug-encapsulated nanoparticles: Towards a novel non-invasive approach to prevent atherosclerosis, Iran. J. Med. Phys. 10 (2) (2013) 118–132.
[29] A. Rowhanimanesh, Towards realization of intelligent medical treatment at nanoscale by artificial microscopic swarm control systems, Int. J. Body Mind Cult. 3 (2017) 9–45.
[30] A. Hajizadeh-S, M.R. Akbarzadeh-T, A. Rowhanimanesh, Dynamic swarm learning for nanoparticles to control drug release function using RBF networks in atherosclerosis, in: 2015 the International Symposium on Artificial Intelligence and Signal Processing, AISP, IEEE, 2015, pp. 112–117.
[31] A. Hajizadeh-S, M.R. Akbarzadeh-T, A. Rowhanimanesh, Swarm learning of interval nanoparticles to estimate the drug release function in atherosclerosis, in: 2015 4th Iranian Joint Congress on Fuzzy and Intelligent Systems, CFIS, IEEE, 2015, pp. 1–5.
[32] N. Yang, K. Vafai, Modeling of low-density lipoprotein (LDL) transport in the artery—effects of hypertension, Int. J. Heat Mass Transfer 49 (5–6) (2006) 850–867.
[33] L.X. Wang, A Course in Fuzzy Systems and Control, Prentice-Hall, Inc, 1996.

S. Sharif is currently a Doctoral Student of Software Engineering at Ferdowsi University of Mashhad. She received her B.S. and M.S. Degrees in Software Engineering in 2009 and 2013, respectively. Her research interests are in the areas of internet of things, cloud computing, nano networks, soft computing and intelligent systems.

S. A. Hossieni Seno is currently an Associate Professor of Computer Engineering at Ferdowsi University of Mashhad. His research interests are in the areas of computer networks, nano networks, sensor-cloud, and internet of things.

A. Rowhanimanesh is currently an Assistant Professor of Electrical Engineering at University of Neyshabur. He received his B.S., M.S., and Ph.D. Degrees in Control Engineering from Ferdowsi University of Mashhad in 2007, 2009, and 2013, respectively. His research interests are in the areas of Intelligent Control, Artificial Intelligence, Systems Biology, and Medical Nanorobotics.